

# Dynamic Simulation of Vertebral Column and Control of the Posture using a Parallel Mechanism

Mouna Souissi<sup>1</sup>, Walid Amokrane<sup>1</sup>, Zefeng Wang<sup>2</sup> and Gerard Poisson<sup>3</sup>

<sup>1</sup>PRISME HEI-Campus centre, 2 Allée Jean Vaillée 36000 Châteauroux, France

<sup>2</sup>FMM HEI-Lille, 13 Rue de Toul 59000 Lille, France

<sup>3</sup>PRISME Laboratory, University of Orléans - INSA CVL, France

**Keywords:** Simulation, Dynamic Brace, Human Spine, Vertebral Column, Mechanical Structure, Kinematics.

**Abstract:** Adolescent Idiopathic Scoliosis (AIS) is a deformity of spine which occurs during growth. This paper presents a novel method for simulation of a 2D and 3D trunk model and the adaptation of an existing parallel mechanism to design parallel joints that can be used to correct abnormal postures of the human spine affected by scoliosis. A 3D model of the system has been elaborated for simulation and design. Simulations results show that this mechanism is able to permit some bending motions of human torso, taking into account the specifications of forward, backward and left/right sideways bending amplitudes.

## 1 INTRODUCTION

### 1.1 Human Spine Description

The human vertebral column extends from the skull to the pelvis and is made up of 33 individual vertebrae (Abbott et al., 2007). These later are stacked on top of each other. They are grouped into four regions (Fig. 1): cervical region, thoracic region, lumbar region, sacrum and coccyx.

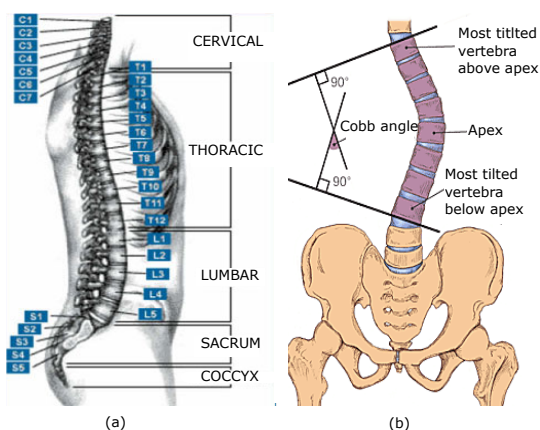


Figure 1: (a) Human Spine. (b) Cobb's angle.

The cervical and lumbar regions enjoy the greatest freedom of movement. In the thoracic region, mo-

tion is limited. Motions of a human spine are characterized by the actuation planes that are the sagittal plane, coronal plane, and axial plane (Fig. 2). The basic movements of the spine can be classified by using planes, as follows:

- In Sagittal plane: Flexion and Extension
- In Coronal plane: Right and Left Lateralization
- In Longitudinal plane: Rotation

Deformity of spine is any abnormality of the formation, alignment, or shape of the vertebral column. Among the existing deformities, the deformation of the spine is due to the scoliosis.

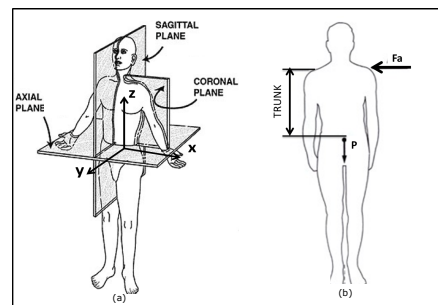


Figure 2: (a) Sagittal plane, coronal plane, and axial plane. (b) Force applied to person to move in sagittal plane.

## 1.2 Spine of the Adolescent Idiopathic Scoliosis (AIS)

A scoliosis curve usually looks a bit like a backward C shape and involves the spine bending sideways to the right, which is also called dextroscoliosis. Side-ways spinal curvature on the left side of the back is more like a regular C shape and called levoscoliosis. Scoliosis is categorized into several types depending on the cause and age of the curve development, 2% to 3% of the population suffer from scoliosis (Anderson, 2007). There are four common types of scoliosis curves: right thoracic curve, right thoracolumbar curve, right lumbar curve, double major curve. The two parts affected by scoliosis are the thorax and lumbar regions.

To measure coronal plane deformity on antero posterior plain radiographs in the classification of scoliosis Cobb angle is used. Cobb angle is defined as the angles formed between a line drawn parallel to the superior endplate of one vertebra above the fracture and a line drawn parallel to the inferior endplate of the vertebra one level below the fracture (Fig. 1).

A diagnosis of scoliosis is confirmed when the Cobb angle, (J. Zhang, 2009) (Behairy, 2000) (Cobb, 1984) (Delorme, 2000), is 10 degrees or greater, which is measured through a standard radiographic examination. x-rays of the entire spine are taken to evaluate the front and side curvature. The Cobb angle is used on x-rays to measure the angle between the most angulated vertebrae that make up the curvature, (Longstein, 1994) (A. H. W. V. Eeuwijk, 2006) (Lafage, 2004). Lines are drawn on the x-rays or a computer program assists to calculate the angle. Most scoliosis curves are between 10 to 40 degrees in magnitude. Although radiographic measurements are used to decide treatment, a small degree of error exists when comparing radiographs. A change of 5 degrees is usually needed to document an actual change in curve progression.

Treatment options for idiopathic scoliosis could include: observation, bracing (Schiller and Ebersson, 2010) (Aulisa and Aulisa, 2014) and surgery. Bracing is the application of external corrective forces onto the spine and trunk. It can be rigid or flexible. But conventional rigid braces present some limitations: difficult to move, lower self-esteem, more fatigue and lower compliance, heavy and non-breathable and uncomfortable.

These braces are designed to be worn 16 to 23 hours a day. And as the child grows, the required external forces to correct the abnormal posture change along the length of the curve and over the course of treatment. Our objective is to achieve a dynamic bra-

ce. It is actuated by 2 motors placed on adjacent rings to control the force or position applied on the human body. In this paper we propose to investigate the kinematics design of a vertebral column for human. Three kinds of experiments are carried out, first experiment of spine in the sagittal plane, second experiment in coronal plane and third experiment in axial plane. Simulations of experiments let to choose the motors of the dynamic brace.

The paper is organized as follows. Section II is dedicated to trajectory planning and inverse kinematics of human model in sagittal plane. Section III proposes a dynamics model for the human spine. Section IV describes the kinematics of the parallel mechanism proposed to correct the posture of spine affected by (AIS). Section V is devoted to conclusion and perspectives.

## 2 TRAJECTORY PLANNING AND INVERSE KINEMATICS OF HUMAN MOTION

### 2.1 Model of Human

A spine is a complex remarkable mechanical structure optimized by thousands generations of humans. It transmits the weight of the upper body to the pelvis and is subjected to internal forces whose magnitudes are many times the entire body weight depicts the human model used for simulation in the sagittal plane  $(y, z)$ . The model is constituted by rectangular segments, namely head, trunk, pelvis, femurs, tibias and arms. Masses and heights of the different body parts are derived from a human kid-size model. Total height is 1.40 [m]. Total mass is  $M_T=40$ [Kg] without pitch joints in the vertebral column.

This mass increases by  $0.01 M_T$  for each pitch joint. The mass of the thorax is equal to the mass of the trunk when the robot has no articulated spine.

Table 1: Masses and heights of body parts.

Part	Masses [Kg]	Height [m]
Head	$0.08M_T$	$0.07H_T$
Arms(2)	$0.1M_T$	$0.47H_T$
Tibias(2)	$0.12M_T$	$0.27H_T$
Thighs(2)	$0.18M_T$	$0.22H_T$
Pelvis	$0.02M_T$	$0.04H_T$
Trunk	$(0.5+0.01\delta_j) M_T$	$0.4H_T$
Pitch joint	$0.01 M_T$	$\frac{1}{12} H_{Trunk}$
Lumbar part	$N_v 0.01 M_T$	$H_{Trunk} - H_{Thorax}$
Thorax	$M_{Trunk}$	$(1 - N_v \frac{1}{12})H_{Trunk}$

Table 1 gives masses and heights of the different parts. The trunk is composed of a thorax and a lumbar part. Foot mass was taken into account in the tibiae. Arms are connected to the shoulders at the top of the thorax.

In order to investigate the influence of the number of vertebrae on pick up an object from the floor, a dynamics study of the model in the sagittal plane was conducted in (M. Souissi, 2011). The motion algorithm uses the pseudo-inverse technique.

The input trajectory to be tracked is defined as

$$F = [x_G, x^{pelvis}, z^{pelvis}, \theta^{pelvis}] \quad (1)$$

Given the input above, the algorithm computes all joint angles ( $\beta^i$ ):

- At  $t=0$ , calculate initial  $\beta_{t=0}^i$ ,  $F_{t=0}$ , and Jacobian  $J_{t=0}$ .
- For each next position  $F_{next}$  of input trajectory,
  1.  $\Delta F \leftarrow F_{next} - F(t)$ .
  2. Calculate pseudo-inverse  $J^+$  from Jacobian  $J$ .
  3.  $\Delta \beta \leftarrow J^+ \Delta F$ .
  4.  $\beta(t + \Delta t) \leftarrow \beta + \Delta \beta$ .
  5. Calculate  $F(t + \Delta t)$  using  $\beta(t + \Delta t)$  from forward geometric model.
  6. Calculate Jacobian  $J$  using  $\beta(t + \Delta t)$  for next step.

Where  $F$  is the force applied by segment  $i$  to  $i - 1$ , and ( $\beta^i$ ) is the joint angle, between segment  $i - 1$  and  $i$ .

## 2.2 Simulation and Results

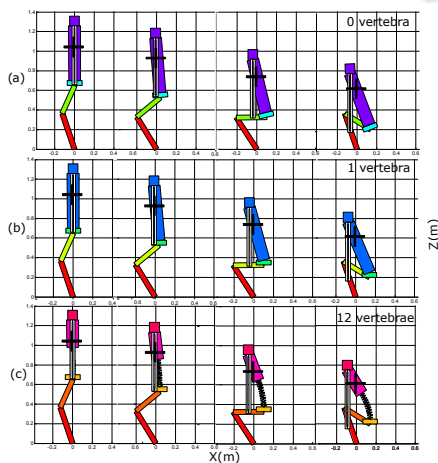


Figure 3: Knee flexion to pick up object on floor. This motion lasts 3 [sec].  $x^{pelvis} = 0.19[m]$  and  $z^{pelvis} = 0.2[m]$ . (a) 0 vertebra, (b) 1 vertebra and (c) 12 vertebrae.

The experiment consists of pick an object from the floor (Fig. 3). This simulation aims to determine the

influence of the number of vertebra pitch joints in matter of sum of work in vertebrae and the inclination of thorax after motion. The cervical region, sacrum and coccyx are fixed. The vertebrae are placed in the lumbar and thoracic region between the first lumbar vertebra and the 7th vertebra of thorax, the region most affected by the (AIS). The experiment was carried out with 0 vertebra, with 1 vertebra and with 12 vertebrae in the spine.

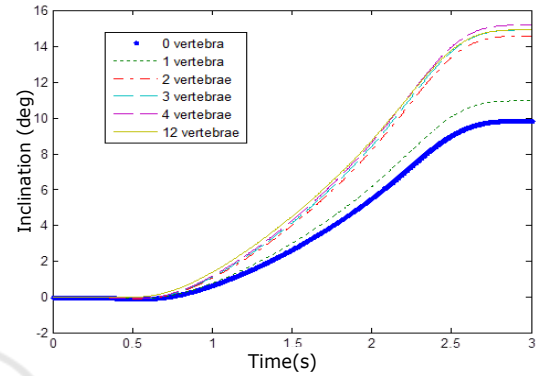


Figure 4: Inclination (degrees) of thorax in flexion of knees to pick up an object from the floor.

Fig. 4 shows the thorax inclination for different number of pitch joints. The inclination of trunk increases significantly when the number of vertebra joints increases. From 12 joints, there is an increase of nearly 50% of thorax inclination compared with the configuration without articulated spine.

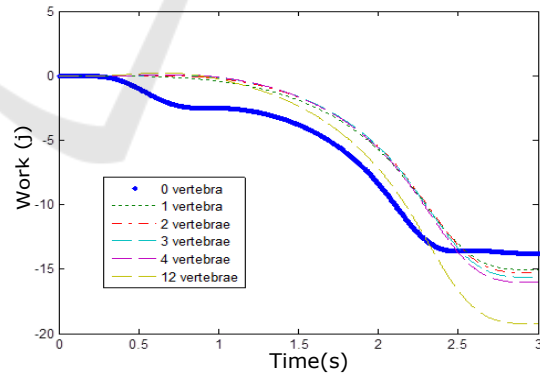


Figure 5: Spine work in the knee flexion.

Fig. 5 shows the work in spine for 0, 1, 2, 3, 4 and 12 vertebrae. The work is less important for a column composed of a single joint. The more vertebrae, the more the work increases. For 12 vertebrae work reaches 19[J].

Simulation experiments carried out in the sagittal plane have shown that pitch joints in the vertebral column is so important. Rigid brace can limit the mo-

tions of kid. According to experiments we propose to work with 12 joints placed in the trunk.

### 3 DYNAMIC SIMULATION OF SPINE

#### 3.1 Dynamics

Fig. 2 shows the actuation planes. In this section the counterclockwise torque  $T_a$  about center of mass produced by the applied force  $F_a$  is calculated:

$$T_a = F_a \cdot L_T \quad (2)$$

Where  $L_T$  is the length of child from center of mass to head and equal to  $0.50[m]$ .

The opposite restoring torque  $T_b$  due to the upper body's weight is:

$$T_b = P \cdot D \quad (3)$$

Where  $D$  is the diameter of waist and assuming that the mass of upper body of the child is  $20[kg]$ , his weight  $P$  is:

$$P = 20 \cdot 9.8 = 196[N] \quad (4)$$

for  $D = 0.101[m]$  and  $T_b = 19.8[N.m]$ . The restoring torque produced by the weight of upper body is therefore  $[N.m]$ . Trunk is on the verge of toppling when the magnitudes of these two torques are equal; that is:

$$T_a = T_b \quad (5)$$

So the force required to move trunk of child in sagittal plane is :

$$F_a = T_a / L_T = 19.8 / 0.30 = 39.6[N] \quad (6)$$

Regarding equation (6) force  $F_a$  depends on the distance between the center of mass and the point of application of force. If  $F_a$  is near of the center of gravity, torque will be so important. And since the center of mass is close to the lumbar part, the force at the level of the lumbar vertebrae is the most important, which explains the dimensions of the vertebrae at this level comparing with the cervical and thoracic vertebrae. For  $L_T = 0.1[m]$ , torque is equal to  $F_a = 198[N]$ . By bending the torso the center of gravity will be shifted away and as the result will the restoring torque be increased.

#### 3.2 A Cad Model for Motion Simulation

In this paper a new model is proposed for the lumbar part of a spine. In this model we consider that all solicitations of the spine are vertically applied at the center of the vertebra. The 3D model has been

elaborated in ADAMS-software with the aim to run a dynamic simulation for computing motion properties and reaction forces (Fig. 6). In ADAMS-software the discus has been modeled as a body that is attached to the assembled vertebrae. Joint between all discs is spherical. This joint is very near to the real type of link between vertebrae.

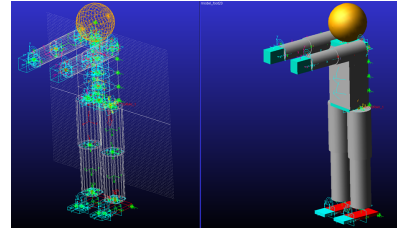


Figure 6: A 3D ADAMS model of all body. Masses and heights of the different body parts are derived from a human kid-size model.

First simulation consists of tilting the entire body to the right and left and calculating the forces applied to the column in the thoracic and lumbar region. Fig. 7 shows the simulation with ADAMS-software and the result of forces applied in vertebrae for the left bending motion. Regarding the simulations, forces applied to the thoracic and lumbar vertebrae vary between  $130[N]$  and  $107[N]$  for the left bending motion. Results correspond to the equation (6). When the distance between force and vertebra is small, the magnitude of force is more important.

Second simulation consists of the forward/backward motion. Fig. 8 shows the simulation with ADAMS-software and the result of forces applied in vertebrae for the forward motion. Forces vary between  $300[N]$  and  $350[N]$ . And third simulation consist of the yaw motion. Forces applied to the vertebrae reaches  $145[N]$ .

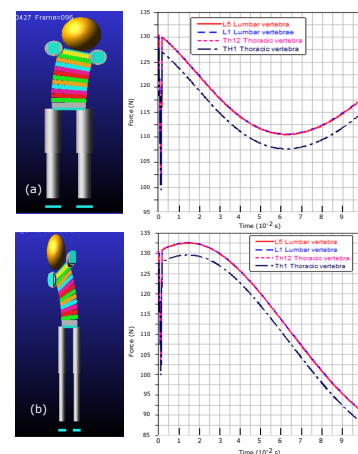


Figure 7: Forces applied to the vertebrae for the left/right bending motion.

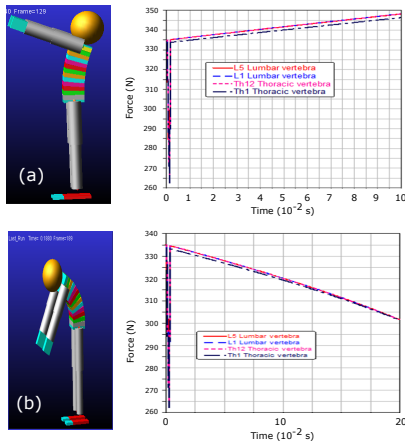


Figure 8: Forces applied to the vertebrae for the (b) forward (c) backward motion.

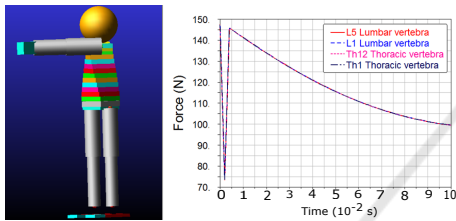


Figure 9: Forces applied to the vertebrae for the yaw motion.

In the next section we propose a parallel mechanism to correct the abnormal posture change along the length of the curve, taking into account the maximal forces applied in vertebrae in the three planes, pitch, roll and yaw motions.

## 4 PARALLEL TILTING MODULE FOR CORRECTING POSTURE

### 4.1 Kinematic Model

In this section we propose a dynamic brace to treat children with scoliosis without limiting upper body movement. Mechanism is fixed close to the vertebrae L1, L2, L3, L4 and L5. This choice is due to the optimization of mechanism in matter of torque applied to the two motors fixed in the bottom platform (M. Souissi, 2016). The objective of this system is to modulate the corrective forces on the spine in desired directions while still allowing the users to perform typical everyday activities. The most important motions to control are the pitch, roll and yaw motions in the actuation planes. Mechanism proposed was simulated with ADAMS. It is fixed in the lumbar region. The parallel mechanism, developed in

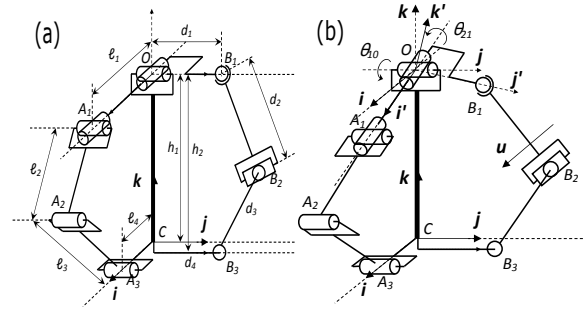


Figure 10: (a) Perspective view of parallel mechanism in initial position. The central rod is fixed and rigid. It is attached to the top platform by a Universal joint at  $O$ . The mechanism is actuated by two revolute joints, each of them is located at the bottom of each arm. The two arms are arranged at  $90 [deg]$ . The arm  $A_1A_2A_3$  is planar and remains in the  $(xz)$  remains in this plane. It is composed of two revolute joints and one U-joint. The other arm  $B_1B_2B_3$  is initially in the  $(yz)$  plane, and does not remain in this plane if the top platform rolls. (b) Perspective view of parallel mechanism after pitch and roll rotations.

(M. Souissi, 2012a) and compared with serial system in (M. Souissi, 2012b), is inspired from a flight simulator (Sabrie, 2004) and (Alexander V. Korobeynikov, ). It consists of 2 platforms – one bottom platform  $CA_3B_3$  and one top platform  $OA_1B_1$ , that are linked by a central vertical rod  $CO$  and two arms arranged at  $90[deg]$  in the initial position (Fig. 10). The central rod  $CO$  is fixed and always remains vertical. It joins the top platform through a Universal joint whose drive is responsible for roll and pitch motion of the top platform. The arm  $A_1A_2A_3$  is planar and is composed of two segments, two revolute joints at  $A_2$  and  $A_3$ , and one Universal joint at  $A_1$ . This is the planar arm. The arm  $B_1B_2B_3$  also includes two segments, one revolute joint at  $B_3$ , one Universal joint at  $B_2$  and one ball joint at the attachment locus  $B_1$  with the top platform. This arm is 3D. The bottom platform is linked to coordinate frame  $R_0$ , centered at  $C$  with axes  $i, j$  and  $k$ . The top platform rotates about  $O$  and is linked to coordinate frame  $R'$ , frame centered at  $O$  whose axes are  $i', j'$  and  $k'$  (Fig. 10). The top platform can be pitched about fixed axis  $j$  by angle  $\theta_{10}$ , and rolled about axis  $i'$  by angle  $\theta_{21}$ .

The two active joints are the revolute joints at  $A_3$  and  $B_3$ . The associated rotation angles are denoted by  $\alpha$  and  $\beta$ .

The length  $d_4$  and  $\ell_4$  are approximately half the lengths  $d_1$  and  $\ell_1$  respectively.

This means that the motor axes should be located in the middle with respect to the trunk half width and the trunk half depth respectively.

Table 2: Normalized parameters of 3D and 2D arm.

Parameter	2D arm	Parameter	3D arm
$\frac{l_1}{h_1}$	2	$\frac{d_1}{h_1}$	1
$\frac{l_2}{h_1}$	0.666	$\frac{d_2}{h_1}$	0.666
$\frac{l_3}{h_1}$	0.733	$\frac{d_2}{h_1}$	0.466
$\frac{l_4}{h_1}$	1.333	$\frac{d_4}{h_1}$	0.666

## 4.2 Torque Considerations

The actuators will have to support the mass  $M$  of the bottom platform. Assuming this mass is concentrated on a point  $G$  that is fixed with respect to the bottom platform, we can express the torques  $\tau_1$  and  $\tau_2$  that the actuators must exert to support this mass:

$$\begin{bmatrix} \tau_1 \\ \tau_2 \end{bmatrix} = J^T \begin{bmatrix} \tau_1^S \\ \tau_2^S \end{bmatrix} \quad (7)$$

where  $J$  is the Jacobian matrix of forward kinematics:

$$\begin{bmatrix} \dot{\theta}_{10} \\ \dot{\theta}_{21} \end{bmatrix} = J \begin{bmatrix} \dot{\alpha} \\ \dot{\beta} \end{bmatrix}$$

$$J = \begin{bmatrix} r_1 & 0 \\ -r_1 r_3 & r_2 \end{bmatrix}$$

$$r_1 = \frac{A_3 A_2}{u_{A_2 A_1} j} O A_1 u_{A_2 A_1} j$$

$$r_2 = \frac{B_3 B_2}{u_{B_2 B_1} i'} O B_1 u_{B_2 B_1} i'$$

$$r_3 = \frac{O B_1}{u_{B_2 B_1} j} O B_1 u_{B_2 B_1} j$$

$$\tau_1^S = M O G g j$$

$$\tau_2^S = M O G g i'$$

where  $g$  is the gravity,  $r_1$ ,  $r_2$  and  $r_3$  are expressed thanks to the scalar triple product of three vectors. The vectors of the type  $u_{XY}$  are unit vectors along the direction given by the pair of points  $X$  and  $Y$ .  $\tau_1^S$  and  $\tau_2^S$  are the gravity torques exerted at the center  $O$  of the bottom platform, respectively about the axis  $j$  and the axis  $i'$ .

Let us give a geometric interpretation. If  $r_3 = 0$ , i.e. actuators are activated separately, we have:

$$\tau_1 = r_1 \cdot \tau_1^S$$

$$\tau_2 = r_2 \cdot \tau_2^S$$

The ratios  $r_1$  and  $r_2$  can be interpreted respectively as the ratio of the area of the triangle  $A_1 A_2 A_3$  over the triangle  $O A_1 A_2$  (Fig. 11), and the ratio of the area of the triangle  $B_1 B_2 B_3$  over the triangle  $O B_1 B_2$ .

To reduce the active torques in the parallel mechanism, it is therefore necessary to reduce these two

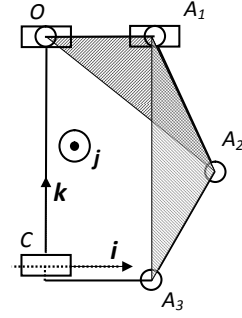


Figure 11: Geometric interpretation of the ratio of the active torque at  $A_3$  over the gravity torque at  $O$ . According to the scalar triple product expression, it is equal to the surface of the triangle  $A_1 A_2 A_3$  over the surface of the triangle  $O A_1 A_2$ .

ratios as much as possible. This can be achieved by a careful choice of the different lengths ( $l_i$ ) of the mechanism, and considering the full scope of inclinations required from the specifications of the tele-echography application. Intuitively through the geometrical interpretation, the surface of the triangle  $A_1 A_2 A_3$  should be reduced compared to the triangle  $O A_1 A_2$ . This can be achieved by increasing the length  $A_1 A_2$  over  $A_2 A_3$ , and increasing the length  $O A_1$  from  $O C$ . However, one may pay attention not to go through flat triangle configurations that represent singularities where the mechanism would not be controllable any more.

The motion consist of giving the angular inputs for the pitch/roll joint of the top platform, namely  $\theta_{10}$  and  $\theta_{21}$ . The vertebral column is bent  $10[deg]$  forward, then  $10[deg]$  backward. The angles for the joint motors, namely  $\alpha$  and  $\beta$  are calculated thanks to the inverse geometric model (Fig. 12).

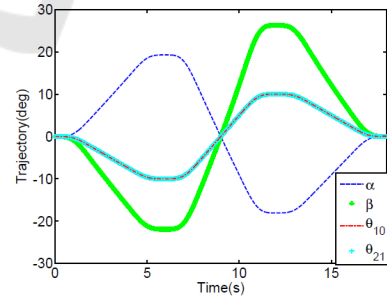


Figure 12: Angle trajectories  $\theta_{10}$  and  $\theta_{21}$  of platform and the related motor angles  $\alpha$  and  $\beta$  for the pitch inclination motion.

## 4.3 Simulations and Result

The prototype was simulated with ADAMS-software and trajectory planning is designed with Matlab-SIMULINK, which is used to control the ADAMS

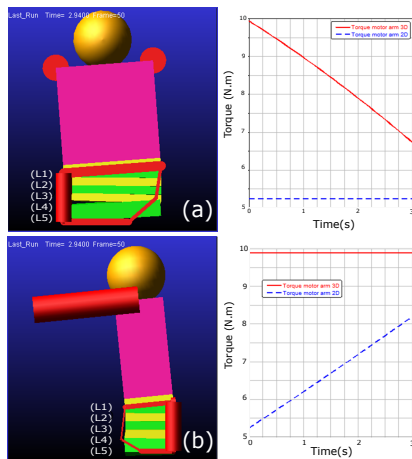


Figure 13: Prototype used to correct the posture in the sagittal(a) and coronal(b) plane.

model (M. Souissi, 2012b), minimization of torque was done in (M. Souissi, 2016). Prototype is used to correct the posture of the spine in two planes: sagittal and coronal plane.

For all experiences done with ADAMS, the sagittal plane is presented by zy-plane, the axial plane is presented by xy-plane and the coronal plane is presented by xz-plane as shown in figure (Fig. 2).

Fig. 13 shows the torque of the two motors of roll and pitch joint to move spine in the sagittal and coronal plane. Maximal torque of the 3D arms is  $10[N.m]$  and torque of the 2D motor is constant and is about  $6[N.m]$  in the first experience. Maximal torque of the 3D arms is  $10[N.m]$  and torque of the 2D motor is constant and is about  $8[N.m]$  in the second experience.

## 5 CONCLUSION AND PERSPECTIVES

In this paper, a model for the human spine is proposed for analyzing applied forces on the intervertebral discs through a suitable motion simulation. A new dynamic brace has been proposed to correct the posture of the human affected by scoliosis in two planes, sagittal and coronal plane. The next steps of this research will consist realization and motorization of system according to the dynamics results obtained.

## REFERENCES

- A. H. W. V. Eeuwijk, S. Lobregt, F. A. G. (2006). A novel method for digital x-ray imaging of the complete spine. 344.
- Abbott, J., Nagy, Z., Beyeler, F., and Nelson, B. (2007). volume 3.
- Alexander V. Korobeynikov, V. E. T. Modeling and evaluating of the stewart platform.
- Anderson, S. M. (2007). Spinal curves and scoliosis, radiologic technology. 79.
- Aulisa, A.G., G. V. M. E. G. M. F. F. and Aulisa, L. (2014). Brace treatment in juvenile idiopathic scoliosis: a prospective study in accordance with the srs criteria for bracing studies-sosort award 2013 winner.
- Behairy, Y., H. D. H. D. M. J. M. M. (2000). Partial correction of cobb angle prior to posterior spinal instrumentation. 20:398–401.
- Cobb, J. (1984). Outline for the study of scoliosis. 5:261–275.
- Delorme, S., L. H. P. B. R. C. C. C. J. (2000). Pre-, intra-, and postoperative three-dimensional evaluation of adolescent idiopathic scoliosis. 13:93–101.
- J. Zhang, E. Lou, L. H. L. D. L. H. J. V. R. Y. W. (2009). Automatic cobb measurement of scoliosis based on fuzzy hough transform with vertebral shape prior. 22:463–472.
- Lafage, V., D. J. L. F. S. W. (2004). 3d finite element simulation of cotredubosset correction. 9:17–25.
- Longstein, J. (1994). Adolescent idiopathic soliosis. 344:1407–1412.
- M. Souissi, V. Hugel, P. B. (2011). Influence of the number of humanoid vertebral column pitch joints in flexion movements.
- M. Souissi, V. Hugel, P. B. (2012a). Design optimization of parallel joint mechanism for humanoid spine. pages 997–1000.
- M. Souissi, V. Hugel, P. B. (2012b). Modeling and simulation of humanoid robot spine vertebra. 2:415–418.
- M. Souissi, V. Hugel, P. B. (2016). Minimized-torque-oriented design of parallel modular mechanism for humanoid waist.
- Sabrie, E. (2004). *Analyse d'un mécanisme de simulation de vol sphérique et son contrôle en temps réel*. Faculté des sciences et de génie universitaire, Laval, Québec.
- Schiller, J.R., T. N. and Ebersson (2010). Brace management in adolescent idiopathic scoliosis. 468:670–678.